ATOMISTIC SCALE STUDY OF LOCAL HEATING IN MOLECULAR DYNAMIC SIMULATIONS DURING NANOINDENTATION INTO SILVER SUBSTRATE

Noraini Abdullah

School of Science and Technology, Universiti Malaysia Sabah
88999 Kota Kinabalu, Sabah, Malaysia

ABSTRACT. *This paper presents an atomistic scale study of the effects of local heating during nanoindentation into silver (Ag). Nanoindentation techniques and experiments with fundamental principles of MD simulations are at first introduced. Classical molecular dynamic (MD) simulations are thus used to simulate the indentation processes, comprising of indentation depths an order of magnitude much smaller than experimental values, and over indentation times several orders of magnitude shorter.A preliminary model of the tip-indenter is introduced and comparisons between a Step-coded and a Ramp-coded MD simulations are also noted. Force-depths curves and snapshots are used to study the effects of local heating. The influence of the indentation speeds and temperature on the deformative behaviour of silver (Ag) are also discussed. Simulation results of nanoindentation into silver also showed that varying indentation speeds will lead to a larger increase in the local kinetic energy and only indentation of slower speeds will exhibit similar results as in the experiments.*

KEYWORDS. Indentation model, nanoindentation, molecular dynamic simulations, indentation speeds

INTRODUCTION

Before the advent of the 19th century, various indentation techniques were used to give a measure of hardness while towards the end of the millenium, various techniques using different types and shapes of indenters were introduced for indentation. However, the exploration of science on the nanometre scale (10^{-9}m) has continued the miniaturisation of technology (Chow and Gonsalves, 1996; Timp, 1999). Materials of nanometre dimensions are now readily employed in many applications and indentation into materials of nanosize dimensions is difficult. Hence the development of new techniques to measure mechanical properties, friction, adhesion and surface topography on the nanometre scale giving rise to the research field of nanotribology. A wide expanding area of nanotribology is nanoindentation which is a technique designed to measure the mechanical behaviour and properties of materials on the nanometre scale (Timp, 1999).

Recent years have seen the advent of nanoindentation testing as the most important probe both in basic research and industrial applications on a variety of materials. Numerous experiments using nanoindentation have identified a remarkable phenomenon, namely that the onset of yielding at the nanoscale, appears to be controlled by homogenous nucleation of dislocation in a small volume of material, especially in metals like Au, Ag, Fe, etc., subject to loads approaching the theoritical

strength, that is, the strength of an ideal or defect-free solid (Mojmir, Martin and Vaclav, 2000).

NANOINDENTATION AND EXPERIMENTAL TECHNIQUES

To determine the mechanical properties of material using modern nanoindentation equipments are relatively easy, however it is quite difficult to understand the mechanics and nature of plastic deformation of materials. Hence, computer simulations based on approaches such as molecular dynamics, offer an ideal and popular approach to investigating numerous questions that arise and cannot be fully explained from experimental nanoindentation measurements, specifically the shape of the force-depth (F-D) curves of the simulations that can be related to specific atomic scale events during indentation. In experiments, the procedure involves pressing a nanosize tip at a constant speed *v* from a given height to a given depth into the surface of a material (loading) and is subsequently retracted to its original position following the same path as for the loading process (unloading). Nanoindentation measurements apply very small penetration forces which result in very small indention depths in the material investigated.

In Situ TEM Method

The in situ technique brings nanoindentation inside the transmission electron microscope (TEM) for in situ mechanical probing.The key benefits using TEM in situ techniques for nanoindentation depend on the abilities to locate the object by TEM imaging, characterise both object and probe by TEM, do mechanical probing of nanoscale objects, measure force-displacement relations, and to study dynamic processes.

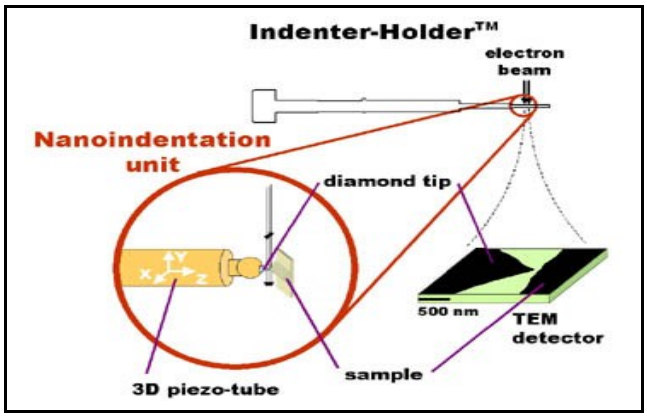

Figure 1. Diagram of Indenter-Holder
(Source: http://www.nanofactory.com/content/insitunanoind.htm)

Locate the object by TEM imaging

TEM imaging enable the tiny sized objects of nanotechnology to be located and allows a local probe to be guided towards a particular object. The diamond tip can be used on many different objects across the sample, for instance, to locate junctions or grain boundaries and place a local probe on the object. This task is difficult or impossible without the power of TEM imaging.

Caracterise both object and probe by TEM
TEM microscopy and microanalysis provide crucial information about both samples and probe microstructures, as well as their shape, separation distance, contact area size, etc. All this information is lacking in standard indentation techniques.

Do local mechanical probing
The force-load relation between the diamond tip and the sample is measured while the sample is being indented. Force curves can be directly correlated to TEM images of the changes in the sample, giving access to the information necessary to understand the mechanical properties of the material.

Study dynamic processes
Before, indentation studies consisted in modifying the sample with bench-top indenter and comparing TEM images taken before and after the indentation. It was not possible to study the whole indentation process since there was no access to the structure changes induced in the sample during the indentation. However, in situ nanoindentation makes it possible to directly observe the whole indentation process with TEM. The atomic structure of the sample can be obtained at all stages of the indentation, while it evolves with time and force-load. In contrast, standard TEM characterisation could be described as imaging of static objects.

Do force imaging using the AFM
The sample can be imaged by running the Indenter Holder™ in atomic force microscope (AFM)-mode just after nanoindentation, providing surface information. While TEM data provides information on the bulk of the sample, AFM gives information on the topography of the surface and its mechanical properties. Nanoindentation experiments performed outside the TEM with an AFM have only access to a two-dimensional image of the sample.

Disclose the unknown sample oxidation
For most metals, oxidation create problems of an unknown factor in the indentation. The fracture of the oxide will show up in the data making it difficult to distinguish from the deformation of the material since the microstructure can only be studied after the indentation. The in situ Indenter-Holder™ solves this problem since TEM imaging reveals whether an oxide layer is present.

MD SIMULATION METHOD

The MD technique is used to model the motion of a system of atoms obeying Newton's Laws. Basically, it has two features, namely the calculations of the atomic forces and consequently, the atomic positions and velocities throughout a specified period of time. In this study, simulations in the order of 10^4 atoms are being employed with a time scale in the order of picoseconds.

Governing Equations of Motion
Considering a system containing N atoms of which the potential energy is the summation of individual atoms, pairs, triplets, etc.

$$V = \sum_i \psi_i(r_i) + \sum_i \sum_{j>i} \psi_2(r_i, r_j) + \sum_i \sum_{j>i} \sum_{k>j>i} \psi_3(r_i, r_j, r_k) \quad (1)$$

The equation of motion is a Lagrangian function, denoted by L and is defined in terms of kinetic energies, K and potential energies, V, as L = K - V. It is considered to be a function of the generalised coordinates, p_k and q_k with their time derivatives, q'_k. The Hamiltonian form of the equation of motion (Bhushan, 1999) can then be defined by the equation:

$$H(p,q) = \sum_k q'_k p_k - L(q, q'_k) \quad (2)$$

In atomic systems, with Cartesian coordinates, r_i and the usual definition of K and V with $F_i = \nabla_{r_i} L = -\nabla_{r_i} V$ being the force on that atom at location r_i, then equation of motion for the *i*th atom will become

$$m_i a_i(t) = F_i \quad (3)$$

where m_i is the mass of atom i and $a_i(t)$, its acceleration .

In an MD simulation, the Born-Oppenheimer approximation is used. In all these simulations, realistic many-body interatomic potentials are used to describe the system and the forces on the tip, calculated by summing the total forces acting on the individual atoms. Examples of potentials used in these simulations are the Ackland'potential (Daw & Baskes, 1984) for the silver-silver (Ag-Ag) interaction, the ZBL potential for the C-Ag interaction (Biersack, Ziegler and Littmack, 1985). The diamond-tip indenter that has a carbon-carbon (C-C) interaction is based on the Brenner potential (Brenner, 1990; Brenner, 1998). Initially adopted by Verlet (1967), this is the most popular method of integrating the equations of motion. The position of every particle i at time t, with time-step, δt can be read as follows:

$$r_i(t+\delta t) = 2r_i(t) - r_i(t-\delta t) + a_i(t)\delta t^2 \quad (4)$$

Here, $a_i(t)$ is calculated using equation (3). The velocities can determine the kinetic energies of the atoms. Swope *et al*. (1982) had proposed a modification of the basic Verlet scheme in which the new position and velocity of atoms at time $t + \delta t$ can be computed as follows:

$$r_i(t+\delta t) = r_i(t) + v_i(t)\delta t + 1/2 a_i(t)\delta t^2, \quad (5)$$

$$v_i(t+\delta t) = v_i(t) + 1/2[a_i(t) + a_i(t+\delta t)]\delta t. \quad (6)$$

This last algorithm is also called as the 'velocity' Verlet algorithm that does not need the storage of the position of atoms at the time of $t - \delta t$. Since the total energy is not exactly conserved for a few MD time steps, it oscillates very closely to a mean value and therefore it can be said that on average the energy is conserved over time scales of a few hundreds of time steps. This algorithm forms the time integration of the atomic coordinates in the MD simulations of this study.

Boundary Conditions

For crystalline materials, boundary conditions are employed to maintain as accurately as possible the realistic physical behaviour of the simulated material. There are typically four types of boundary conditions that can be imposed on the atoms in the system and are specific to the kind of phenomenon under study. Free boundary

conditions are usually applied when there are no restrictions on the dynamics of the atoms while fixed or rigid boundary conditions can be applied to edge atoms to constrain the vertical or horizontal motion of the atoms. Edge effects can be reduced by employing periodic boundary conditions (PBCs) that allow edge atoms to interact with those on the opposite side of the lattice.

Boundary conditions are used to control the temperature of the system by simulating effectively the dissipation of energy through the bulk. There are other numerous thermostats available to damp the motion of selected atoms. More sophisticated ones are achieved by Langevin dynamics, besides the Berengsen equations of motion (Berengsen & Gunsteren, 1985) and the Nosé–Hoover thermostat (Hoover, 1986). Periodic boundary conditions (PBCs) are applied to all the side atoms of the substrate while all the other atoms were allowed to move with the MD algorithm. The silver substrates were indented initially, at first without temperature, that is, damped and later, the materials were thermalised with temperature added to the system by a heat bath until 300K. Then, the heat bath is removed and thermalisation only occurs at the sides of the substrates during indentation. This is done so that the heat generated during indentation when the atoms are damped and thermalised can be distinguished. The damping model is not based on any concept of temperature control and for simplicity the Lindhard-Scharff inelastic loss model (Lindhard *et. al*., 1963) is used. Figure 2 below shows a diagram of the substrate condition.

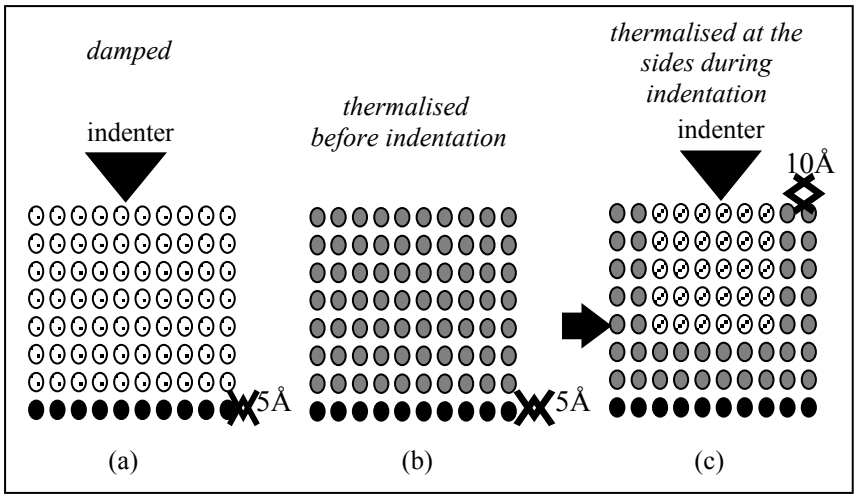

Figure 2. A schematic diagram of substrate conditions utilised in the nanoindentation simulations. The black shaded atoms denote 5Å of fixed atoms, (a) dotted - damped atoms, (b) grey - thermalised atoms at 300K before indentation, and (c) striped - thermalised atoms 10Å above the fixed atoms and round the sides of lattice only during indentation.

Thermalised Atomic Motion's Equations

The temperature of the systems of many physical conditions may be held fixed rather than conserve the total energy. This can be achieved by maintaining the system in contact with a thermal bath. The atoms then follow a random motion similar to that described by the Brownian movement, that is, small particles of colloidal size immersed in a fluid colliding with the microscopic particles of the fluid. The equation of motion for a particle i immersed in a fluid is given by the Langevin equation

(Doob, 1942):

$$ma_i(t) = F_i - \beta r_i'(t) + \Gamma_i(t) \tag{7}$$

of which three different terms are clearly distinguished, that is: i) the first term is related to the interatomic interactions, ii) the second term representing a dynamical friction due to the viscosity of the surrounding fluid, and iii) one stochastic part which is the characteristics of the Brownian motion and has a zero mean, that is, $\langle \Gamma_i(t) \rangle = 0$.

In the case of a system in thermal contact with a heat bath, the direction and velocity of the particles are continuously being modified by the exchange of phonons between the system and the heat bath. Therefore phonons play the same role in the Brownian motion as that of the microscopic particles immersed in a fluid. This also applies for a system whose temperature is held fixed. Because of the stochastic terms in the Langevin equation, it cannot be derived from a conservative Hamiltonian method. However, Ermack (1976) had developed an algorithm to conduct 'Brownian dynamics' simulation by which the position and velocity at a time t can be advanced as follows:

$$r_i(t+\delta t) = r(t) + c_1 v_i(t)\delta t + c_2 a_i(t)\delta t^2 + \delta r_i^G \tag{8}$$

$$v_i = c_0 v_i(t) + (c_1 - c_2)a_i(t)\delta t + c_2 a_i(t+\delta t)\delta t + \delta v_i^G \tag{9}$$

where the values of the coefficients are :

$$c_0 = e^{-\alpha \delta t} \tag{10}$$

$$c_1 = (\alpha \delta t)^{-1}(1 - c_0) \tag{11}$$

$$c_2 = (\alpha \delta t)^{-1}(1 - c_1) \tag{12}$$

and δr_i^G and δv_i^G are random variables sampled from a bivariate Gaussian distribution (Chandrasekar, 1943). These last terms of the Langevin equation are chosen from a random distribution, hence there is not a unique trajectory similar to a conventional MD simulation. By varying the sequence of random numbers δr_i^G and δv_i^G, different trajectories can be simulated. However, these simulations would all led to the same thermodynamics averages after a sufficiently long time.

The nanoindentation of the Ag substrates as a function of the indentation speed, *v* was first run using a Step-code for all the speeds and later run using a better Ramp-code which allows the slowing down of the indenter just before and after maximum indentation during loading and unloading. A schematic diagram of the Step- and the Ramp-MD code velocity profiles are shown in Figures 3 and Figure 4.

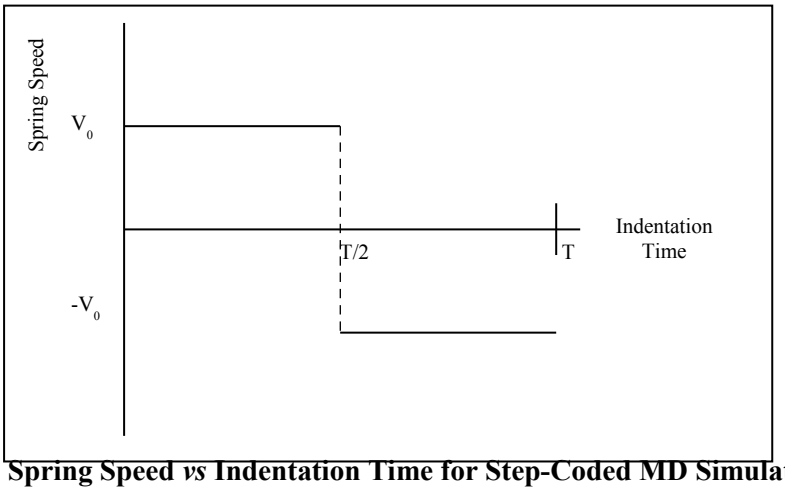

Figure 3. Spring Speed *vs* Indentation Time for Step-Coded MD Simulations

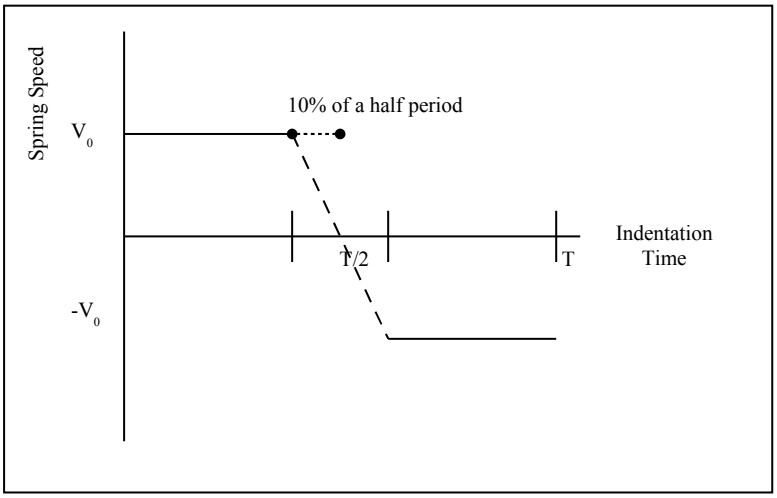

Figure 4. Spring Speed *vs* Indentation Time for Ramp-coded MD simulations

With the Step-code, the indenter moves with the indentation speed until maximum indentation that occurs at half period (T/2) and then it is being retracted abruptly without allowing any relaxation time or slowing down of the indenter. As with the Ramp-code, the indenter as before, moves with the indentation speed but starts to reduce speed or gain retraction speed at about 10% on either side of a half period (T/2), that is, before and after maximum indentation depth to allow for the indenter to indent or retract without any strong vibrations of the cantilever.

MD SIMULATION RESULTS

Silver Ag (101) substrate

The workspace parameters employed for the Ag substrates are depicted in Table 1. The simulation times run from a few hours to a few days and goes on even to a few weeks for slow indentation speeds. All the simulation snapshots pictures presented are

produced using certain software packages such as VTK (http://www.kitware.com/vtk) to allow atomistic snapshots to be viewed at specific periods of time. In the snapshots, atoms are presented as spheres and coloured according to their local heating, corresponding to the temperature of the atoms.

Table 1. Workspace and simulation parameters for silver substrate

Substrate Material	Silver	
Substrate crystal structure	Fcc	
Workspace dimensions	65Å x 65Å x 65Å(001) surface	16384 atoms (1647tip atoms)
Indenter directions	[001]	
Indenter speeds	1m/s to 50m/s	
Substrate temperature	Damped (zero K); Thermalised (300 K)	
MD time step	1.00 fs	

Figures 5, Figure 6 and Figure 7 present a series of force-depth curves at varying damped speeds of maximum indentation and retraction into Ag substrate using the Ramp-code. The upper portion of the curves correspond to the loading stage and the lower portion is the load during extraction. With reference to the force-indentation depth curves (let say for 50m/s) the thermalised speed has a bigger gradient from –5 to 0 indentation depth, that is, before indentation into the substrate. This feature is obvious in all the force-depth curves for all speeds except for 1m/s when the thermalised speed then has a smaller gradient than the damped.

However, as indentation proceeds further into the substrate of depth approximately between 0-12Å the force gradually increases upwards in a slope with several small peaks or 'pop-ins'. These 'pop-ins' are distinct with slower indentation speeds as shown in subsequent curves for 10, 5 and 1m/s. In all the simulations, the indenter reached a maximum penetration depth of approximately 14Å. The peak force acting on the dimensional tip is approximately 113.0 eV/Å which occurred just before the maximum indentation depth at approximately 9.0-12.0Å.

On retraction, the force acting on the indenter quickly declines due to the occurrence of appreciable plastic deformation. Contrary to loading during indentation, the slope during unloading shows similar shape and gradient for all speeds. However, the slope during unloading is much gentler at slower indentation speeds. The elastic recovery of Ag takes place over approximately 6.0Å depth for all speeds. The load-displacement curves also show that the tip is compressed by roughly 2.0Å during indentation. The elastic recovery of the substrate compares very well between the force-depth curves for all speeds, damped and thermalised. This is expected since the elastic recovery of the work material is centered on the indentation region. The series of graphs from the above figures also show that the force-depth curves have similar shapes for all the respective damped and thermalised speeds.

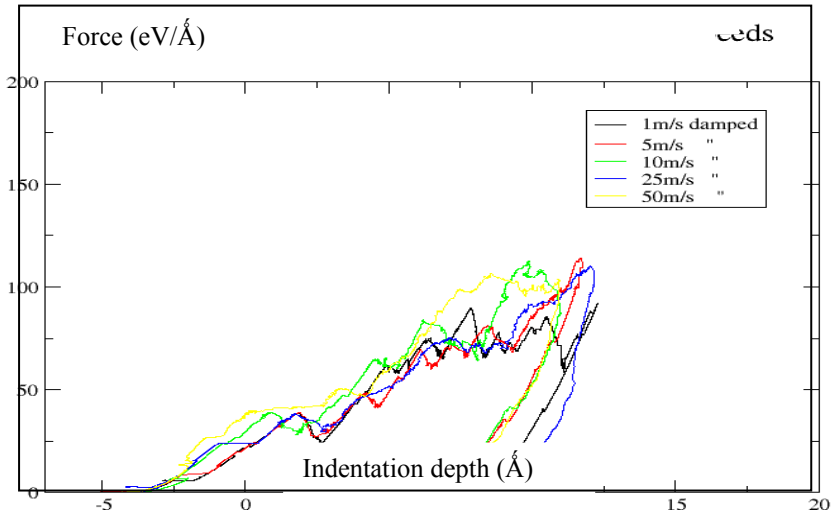

Figure 5. Force-identation depth curves with damped indentation speeds

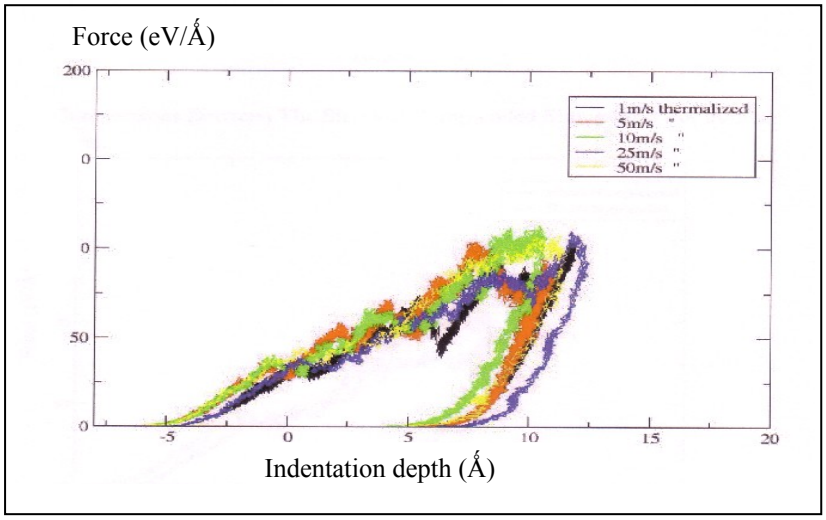

Figure 6. Force-identation depth curves for thermalised indentation speeds

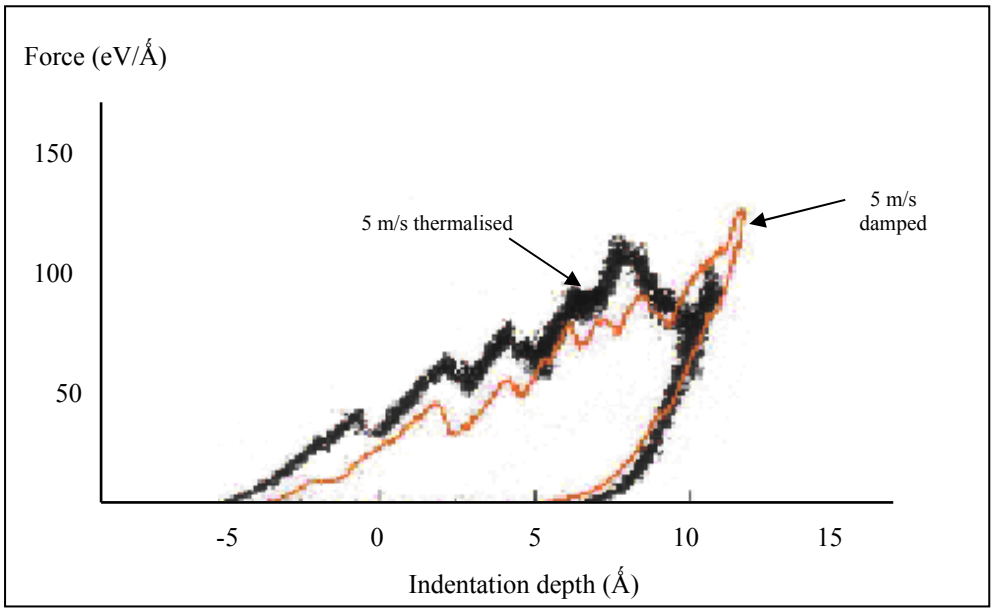

Figure 7. Force-indentation depth curves for 5m/s (thermalised and damped)

Figure 8 compares the spring-force versus indentation time using the Step and Ramp-codes for thermalised indentation speed of 50m/s. For slower indentation speeds, Ramp-coded simulation was found to be able to eliminate the spring force vibrations during the unloading of the indenter during nanoindentation.

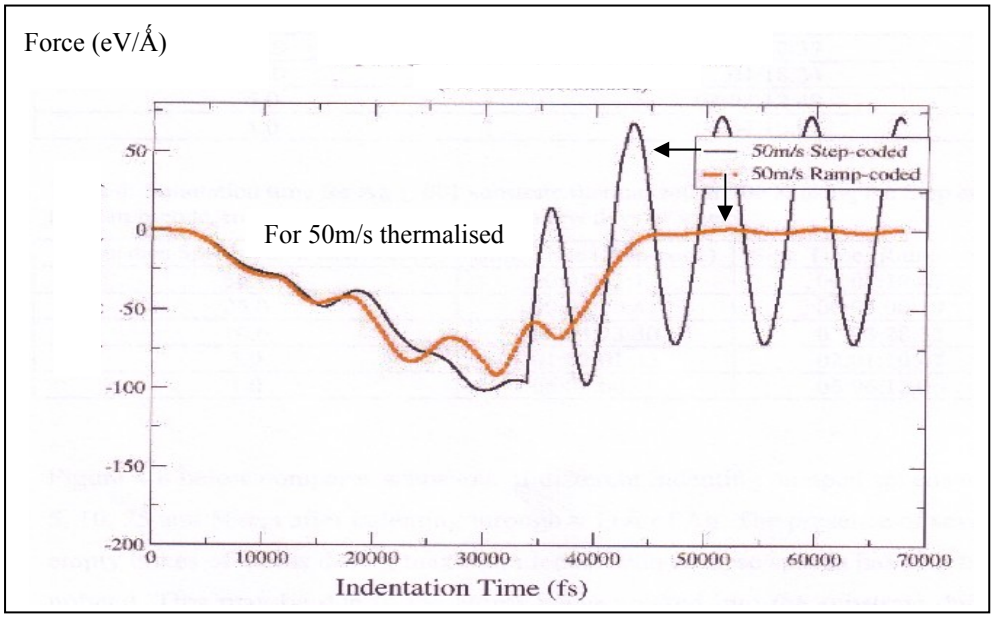

Figure 8. Spring Force *vs* Indentation Time

At different indentation speeds of 1, 5, 10, 25 and 50m/s, the presence of several empty boxes of atoms during maximum indentation at these damped speeds has also been noticed. This may be due to the atoms being pressed into the substrate during indentation. For indentation speed from 50 to 1m/s in the temperature range of

0 to 150K, the number of heated atoms also decreases as the indentation speed decreases. At slower speeds such as 1m/s, the presence of heated atoms has dropped to zero indicating that the thermostat has successfully dissipated the heat generated during indentation.

Snapshots of simulations of all thermalised speeds at maximum indentation times from 0 to 700K have been taken, showing that for the thermalised simulations, the number of heated atoms is more than the respective damped simulations and also the number also decreases as the indentation speed decreases. Figures 9 and Figure 10 compare snapshots of indentation damped and thermalised speeds of 5m/s after indentation through ≈ 11Å of Ag.

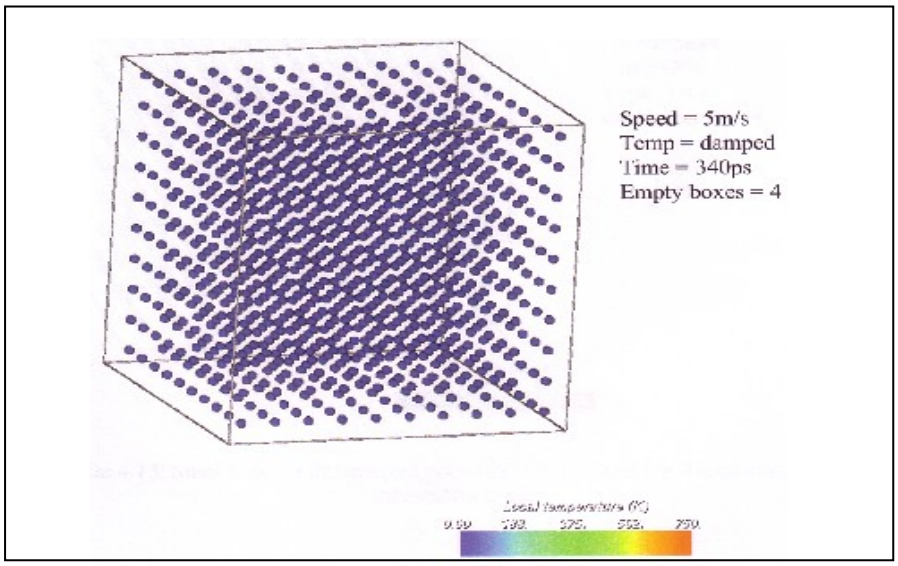

Figure 9. Snapshot of damped simulations at 5m/s

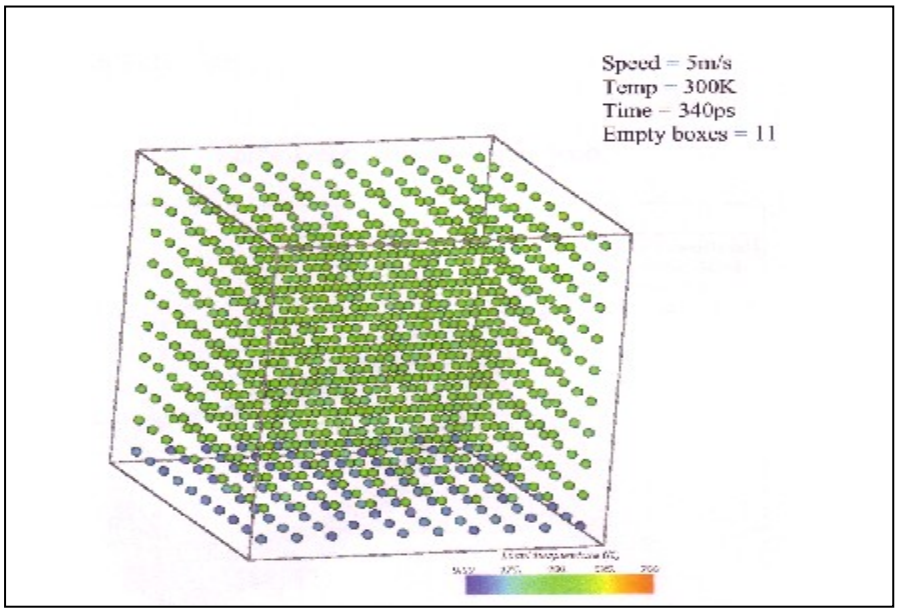

Figure 10. Snapshot of thermalised simulations 5m/s

DISCUSSIONS

With higher indentation speeds, the force–depths curves show 'pop-ins' with small peaks for both damped and thermalised atoms of the Ag {101} substrates whereas with slower indentation speeds, the 'pop-ins' are quite pronounced with higher peaks. For silver, all the curves also show a marked drop from the maximum peak force of approximately 113eV/Å while the indenter is unloading, that is, when retraction occurs. The slopes during unloading are of similar shapes and gradients with a gentler slope at slower speeds. This is because during a sudden retraction of the indenter from Ag, with a simulation of a higher indentation speed (say 50m/s), the cantilever which is attached to a spring will experience vibrations due to this phenomenon. These indentations are initially simulated using a Step-coded MD simulations which are later replaced using the Ramp-code so as to reduce the spring force vibrations and this is achieved by running the indenter at a slower speed, approximately 10% of the half period, just before and after maximum indentation depth during loading and unloading.

Ramp-coded simulation curves also produce distinct 'pop-ins' during loading and gentler slope during unloading at slower indentation speeds. Hence, nanoindentation simulations are better simulated using the Ramp-code. However, simulations with 5m/s seem to produce nearly exact curves at both loading and unloading stages when both codes are used implying that future simulations is best run at this speed. The elastic recovery of Ag compares well for both the damped and thermalised speeds. Snapshots of the simulations in Ag show that the number of heated atoms decreases with slower indentation speeds for both damped and thermalised.

CONCLUSIONS

Nanoindentation MD simulations have provided fundamental insights with the atomic processes underlying nanometric heating of the single-crystal silver. Nanoindentation procedures comprises of two steps: indentation of the substrates with specified speeds followed by the retraction of the indenter. Initially, indentation is done with an abrupt retraction using a Step-coded MD simulation but later with a better Ramp-coded simulation so as to eliminate the spring force vibrations during the unloading of the indenter. During nanoindentation, there is a local region of higher temperatures for both damped and thermalised cases. As for the thermalised atoms in Ag, there are also regions of dispersed heated atoms in the layers of lattices below the indentation region. This is so due to the heat generated during indentation being dissipated through the lattice to regions far from the actual indent. Higher indentation speeds also lead to a larger increase in local kinetic energy or local temperature below the indenter and in the substrates. At slower indentation speeds (1 to 5m/s) the temperature below the indenter is lower. The presence of empty boxes during maximum indentation and after retraction also varies with the corresponding indentation speeds. During unloading (retraction) for silver, only slower speeds will exhibit similar results as in the experiments. For future work it is recommended that indentation speed of 5m/s is best used in nanoindentation MD simulation.

REFERENCES

Berendsen, H.J.C. & van Gunsteren, W.V.1985. Molecular Dynamics simulation of statistical mechanical systems. *Soc.Italiana di Fisica*: pp.43.

Brenner, D.W.,1990. Empirical potential for hydrocarbons for use in simulating the chemical vapour deposition of diamond films, *Phys. Rev. B*, **42**:9458.

Brenner, D.W., 1998. Molecular Dynamics simulations of Atomic-Scale Friction of Diamond Surfaces. *Phys. Rev. B,* **46**, 9700.

Daw, M.S. & Baskes, M.I., 1984. Embedded-atom Method: Deviation and application to impurities, surfaces, and other defects in Metals. *Phys.Rev.B*, **29**(12):6443-6453.

Verlet, L., 1967. Computer experiments on classical fluids.I.Thermodynamical properties of Lennard-Jones molecules. *Phys. Rev*., **159**:98-103.

Swope, W.C., Anderson, H.C.,Berens, P.H. & Wilson, K.R.,1982. Velocity Verlet Algorithm: Molecular Dynamics. *J. Chem.Phys*., **76**:637.

Lindhard, J., Scharff, M. & Schiott, H.E.,1963. Range Concepts and Heavy Ion Changes. *K.Dan Vidensk Selsk. Mat. Fys.Medd*. **33**(14):1-42.

Visualization Tool Kit (VTK), Kitware Inc.,28 Corporate Drive, Clifton Park, New York, 12065 USA. http://www.kitware.com/vtk